

Engineering and Rewiring of a Calcium-Dependent Signaling Pathway

Maja Meško,^{||} Tina Lebar,^{||} Petra Dekleva, Roman Jerala,* and Mojca Benčina*

Cite This: *ACS Synth. Biol.* 2020, 9, 2055–2065

Read Online

ACCESS |

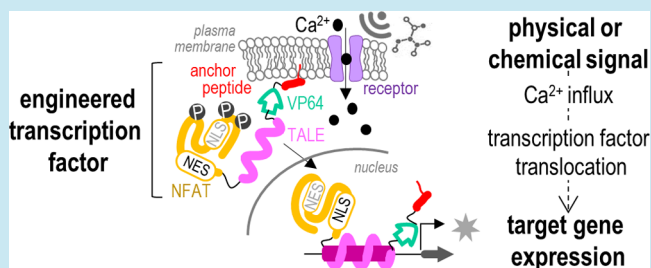
Metrics & More

Article Recommendations

Supporting Information

ABSTRACT: An important feature of synthetic biological circuits is their response to physicochemical signals, which enables the external control of cellular processes. Calcium-dependent regulation is an attractive approach for achieving such control, as diverse stimuli induce calcium influx by activating membrane channel receptors. Most calcium-dependent gene circuits use the endogenous nuclear factor of activated T-cells (NFAT) signaling pathway. Here, we employed engineered NFAT transcription factors to induce the potent and robust activation of exogenous gene expression in HEK293T cells. Furthermore, we designed a calcium-dependent transcription factor that does not interfere with NFAT-regulated promoters and potently activates transcription in several mammalian cell types. Additionally, we demonstrate that coupling the circuit to a calcium-selective ion channel resulted in capsaicin- and temperature-controlled gene expression. This engineered calcium-dependent signaling pathway enables tightly controlled regulation of gene expression through different stimuli in mammalian cells and is versatile, adaptable, and useful for a wide range of therapeutic and diagnostic applications.

KEYWORDS: nuclear factor of activated T-cells, calcium signaling, nuclear export signal, membrane anchoring peptide, transcription activator-like effectors, TRPV1 ion channel



The regulation of gene expression, guided by endogenous stimuli, is a valuable tool for cell reprogramming and cell-based gene therapy. Synthetic circuits have the potential to orchestrate protein expression and cellular physiology and provide the means to precisely regulate the expression of exogenous and endogenous genes. Synthetic biology has advanced the design of gene circuits¹ that are responsive to various external signals, such as small molecules, light, radio-waves, and temperature.^{2–5} Engineered transcription factors, based on designed DNA-binding domains such as transcription activator-like effectors (TALEs) or clustered regularly interspaced short palindromic repeats (CRISPR), can target an almost unlimited number of DNA targets, making them a powerful tool for the regulation of virtually any selected gene.^{6–12} When coupled with inducible systems, designable transcription factors enable the external control of gene expression.^{13–15}

Calcium-dependent transcription factors are attractive tools for synthetic biology applications, as many different physical and chemical stimuli can induce the cellular uptake of calcium ions by activating a variety of membrane receptors, such as G-protein coupled receptors and calcium-selective ion channels.¹⁶ Most calcium-dependent synthetic gene circuits engineered to date in eukaryotic cells harness the nuclear factor of activated T-cells (NFAT) signaling pathway.^{3,4,17,18} NFAT is a central transcription factor in mammalian cells that is regulated by calcium influx *via* activation of the calcineurin phosphatase,

which in turn dephosphorylates NFAT. This modification results in the translocation of NFAT from the cytosol to the nucleus, where it regulates gene expression.^{19,20} An optogenetic approach has been reported that exploited calcium signaling for the activation of NFAT-regulated transgenes and endogenous genes in mammalian cells,²¹ while other successful attempts at external NFAT regulation include the use of stimuli such as fatty acids,²² radio-waves,³ ultrasound,²³ and menthol.⁴ NFAT-regulated exogenous gene expression has also been demonstrated *in vivo* in hypercalcemic mice.²⁴

The activation of transgene expression by exploiting the endogenous NFAT transcription factor is usually weak in cell types with low levels of native NFAT expression. Here, we overexpressed NFAT in HEK293T cells to enhance the activation of an exogenously introduced gene. We found that NFAT overexpression results in its constitutive translocation and transcriptional activity in the absence of calcium influx. To enable potent NFAT activity while maintaining tight control, we prepared engineered NFAT variants with modified

Received: March 5, 2020

Published: July 6, 2020



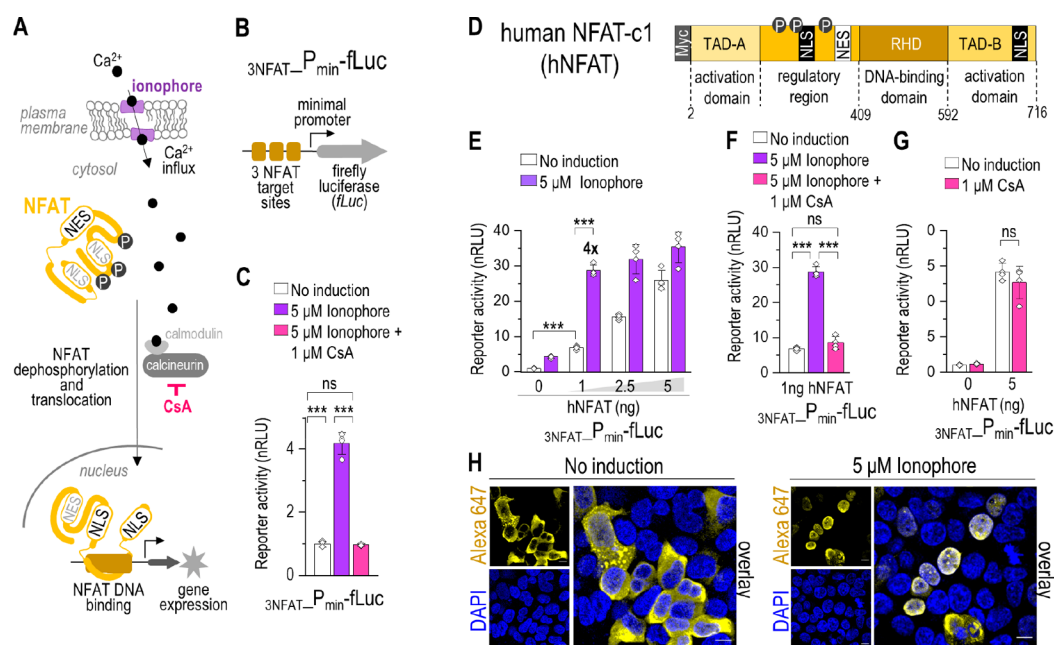


Figure 1. Overexpressed NFAT constitutively activates transcription in HEK293T cells in the absence of calcium influx. (A) Schematic presentation of the calcineurin/NFAT signaling pathway. An external signal (e.g., ionophore) triggers calcium influx. Calmodulin binds calcium ions and activates the calcineurin phosphatase, resulting in NFAT dephosphorylation. This is followed by translocation of NFAT to the nucleus, DNA binding, and activation of gene expression. The activity of calcineurin is inhibited by cyclosporine A (CsA). (B) Schematic presentation of the $3_{NFAT_P_{min}}\text{-fLuc}$ reporter plasmid. (C) The native calcineurin/NFAT signaling pathway in HEK293T cells mediates the weak activation of reporter gene expression. (D) Schematic presentation of the hNFAT construct with a N-terminal Myc tag. The human NFAT-c1 isoform contains two transactivation domains (TAD-A and TAD-B), the RHD (Rel-homology domain) DNA-binding region, and a regulatory region with phosphorylation sites and localization signals. (E) Overexpressed hNFAT enhances reporter gene expression in both stimulated and nonstimulated HEK293T cells, with a maximum of a 4-fold difference between the stimulated and nonstimulated cells. (F) calcineurin/NFAT signaling mediates the ionophore-induced activation of reporter expression in HEK293T cells transfected with the hNFAT-encoding plasmid. (G) The constitutive hNFAT transcriptional activity in nonstimulated HEK293T cells is not mediated by calcineurin activity. (H) Confocal microscopy images of HEK293T cells transfected with 100 ng of the hNFAT encoding plasmid. The images were acquired 1 day after transfection following 3 h of cultivation with or without ionophore and immunostaining with DAPI, anti-Myc tag primary antibodies, and Alexa 647-conjugated secondary antibodies. The scale bars represent 10 μ m. Amounts of transfected plasmids for all luciferase experiments are listed in Table S1. One day after transfection, cells were stimulated with ionophore or both ionophore and CsA. Reporter activity was measured 6–8 h after treatment. The bars represent the mean \pm s.d.; $n = 4$ biologically independent cell cultures. Statistical analyses and the corresponding p -values are listed in Table S2.

subcellular localization properties. Furthermore, the native NFAT DNA-binding domain was replaced with a designed TALE DNA-binding domain and the VP64 activation domain. This replacement ensured efficient calcium-dependent activation of target transgene expression in several mammalian cell types. Replacement of the DNA-binding domain also eliminated off-target activation of NFAT promoter-driven gene expression, implying that the engineered NFAT-TALE chimera does not interfere with autologous NFAT-regulated genes. Moreover, coupling of the circuit to a signal-sensing ion channel resulted in temperature- and small molecule-controlled activation of transgene expression. The engineered NFAT-based transcription factors characterized here are suitable for a range of therapeutic and diagnostic applications, as the calcium-dependent circuit can be coupled to diverse calcium signal transducing receptors.

RESULTS AND DISCUSSION

Overexpressed NFAT Triggers Constitutive Transcription in HEK293T Cells. Calcium signaling represents an attractive regulatory mechanism for use in engineered biological circuits, as the influx of calcium ions can be triggered by a plethora of chemical and physical signals. Calcium influx in mammalian cells is coupled to transcriptional control *via* the NFAT transcription factor, which regulates gene expression in

response to increased intracellular calcium levels. Our initial aim was to harness the native NFAT transcription factor for the transcriptional regulation of exogenously introduced genes in HEK293T cells (Figure 1A). Cells were transfected with a firefly luciferase reporter plasmid containing three NFAT binding sites upstream of a minimal promoter ($3_{NFAT_P_{min}}\text{-fLuc}$) (Figure 1B). To trigger calcium influx, cells were stimulated with the A21387 calcium ionophore (hereafter referred to as “ionophore”). An ionophore is an ion-carrier that conducts calcium ions through a lipid membrane without the need for a protein pore, mimicking diverse cellular processes that result in calcium influx. Stimulation of cells with ionophore resulted in weak but significant activation of reporter gene transcription (Figure 1C, Figure S1). The poor response was not improved by varying the reporter plasmid amounts or ionophore concentration (Figure S1). Nevertheless, the ionophore-mediated transcriptional activation was reduced to background levels by the calcineurin inhibitor cyclosporine A (CsA), confirming that the modest response did indeed occur through the canonical calcineurin/NFAT signaling pathway (Figure 1C).

As response strength is essential for the efficient performance of engineered biological circuits, we aimed to increase the amplitude of the response. To enhance NFAT-mediated transcriptional activity, we overexpressed a Myc-tagged

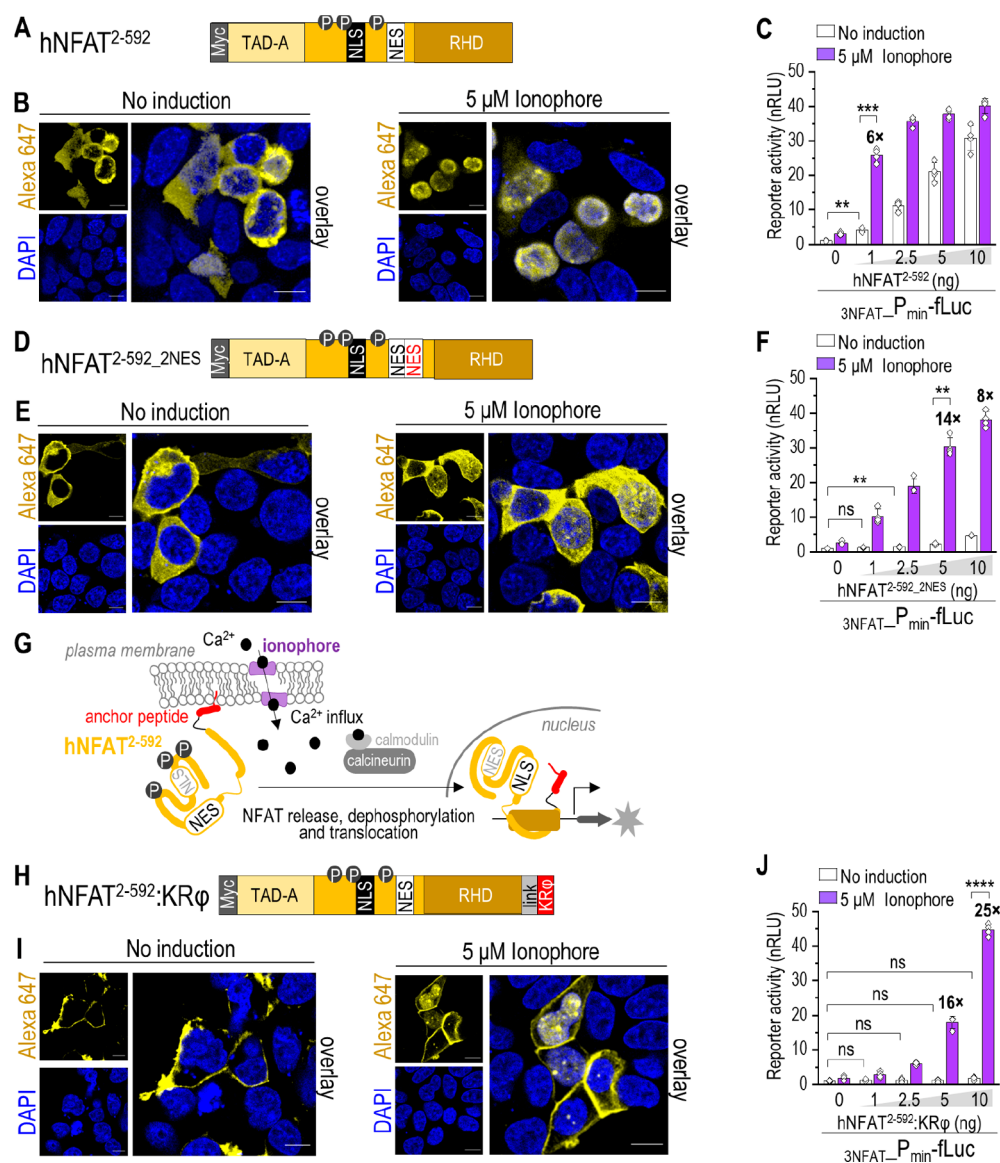


Figure 2. Engineered NFAT variants with modified localization exhibit reduced constitutive activity in the absence of calcium influx. (A) Schematic presentation of an engineered NFAT variant with a truncated C-terminal transactivation domain (hNFAT²⁻⁵⁹²). (B) Confocal microscopy images of HEK293T cells expressing the hNFAT²⁻⁵⁹² construct. (C) The truncated hNFAT²⁻⁵⁹² enhances luciferase reporter gene expression in both stimulated and nonstimulated HEK293T cells. (D) Schematic presentation of an engineered NFAT variant with a truncated C-terminal transactivation domain and an inserted nuclear export signal (NES) (hNFAT^{2-592_2NES}). (E) Confocal microscopy images of HEK293T cells expressing the hNFAT^{2-592_2NES} construct. (F) The hNFAT^{2-592_2NES} construct mediates reduced constitutive activity in nonstimulated HEK293T cells with up to a 14-fold change in luciferase reporter expression following stimulation with ionophore. (G) Schematic presentation of the expected localization of a membrane anchor peptide-tagged hNFAT²⁻⁵⁹² construct. In the absence of calcium influx, the peptide anchors NFAT to the plasma membrane. Following ionophore stimulation and increased cytosolic calcium levels, the peptide is released from the plasmalemma and is included in the calcineurin/NFAT signaling pathway. (H) Schematic presentation of an engineered NFAT variant with a truncated C-terminal transactivation domain and an added membrane anchor peptide (hNFAT²⁻⁵⁹²:KRφ). “Link” represents a flexible linker peptide. (I) Confocal microscopy images of HEK293T cells expressing the hNFAT²⁻⁵⁹²:KRφ construct. (J) The hNFAT²⁻⁵⁹²:KRφ construct exhibits no significant transcriptional activity in nonstimulated HEK293T cells, with a 25-fold change in luciferase reporter expression following ionophore stimulation. For confocal microscopy experiments, HEK293T cells were transfected with 100 ng of the NFAT variant-encoding plasmid. All confocal microscopy images were acquired 1 day after transfection following 3 h of cultivation with or without ionophore and immunostaining with DAPI, anti-Myc tag primary antibodies, and Alexa 647-conjugated secondary antibodies. The scale bars represent 10 μm. The amounts of transfected plasmids for all luciferase experiments are listed in Table S1. One day after transfection, cells were stimulated with ionophore. Reporter activity was measured 6–8 h after treatment. The bars represent the mean ± s.d.; *n* = 4 biologically independent cell cultures. Statistical analyses and the corresponding *p*-values are listed in Table S2.

human NFAT-c1 isoform (hereafter referred to as hNFAT) (Figure 1D). Although hNFAT overexpression markedly increased the expression of the luciferase reporter in ionophore-stimulated cells, reporter activity was also significantly increased in uninduced cells, which was unexpected

(Figure 1E). Nevertheless, the differences between non-stimulated and stimulated cells were significant and reached up to 4-fold increase in reporter gene expression (Figure 1E). Incubation of transfected HEK293T cells with both ionophore and the CsA inhibitor reduced hNFAT transcriptional activity

to the level of uninduced cells (Figure 1F), confirming that the ionophore-triggered response is due to calcineurin/NFAT pathway signaling. Surprisingly, when the hNFAT-expressing cells were incubated with CsA in the absence of ionophore, we did not find significant inhibition of the hNFAT-mediated constitutive reporter expression (Figure 1G), suggesting that the undesired hNFAT activity in uninduced cells is independent of the calcineurin pathway. Confocal microscopy results revealed the partial nuclear localization of hNFAT in uninduced cells, with robust ionophore-triggered translocation of the cytosolic fraction to the nucleus (Figure 1H). In agreement with these findings, it was previously reported that a fraction of the native NFAT constitutively localizes to the nucleus of regulatory T-cells in a calcineurin-independent manner.²⁵ It is speculated that this might be due to the action of other phosphatases,²⁵ however, it is possible that other post-translational modifications, such as acetylation, could also have an effect on NFAT localization and activity.²⁶ The observed phenomenon presents a major concern for the use of hNFAT in engineered cellular circuits, as tight regulation is critical for their use in therapy, diagnostics, and other applications. This tight control is especially important for synthetic circuits of higher complexity with several layers of regulation, where the undesired activity of a single component can greatly reduce circuit functionality.

Engineering NFAT Variants with Modified Subcellular Localization Properties. To construct a stringent calcium-dependent transcription factor with minimal activity in the uninduced state, we focused on engineering hNFAT by modifying its localization properties. To achieve this goal, hNFAT needs to be driven out of the nucleus in the uninduced state, while maintaining its ability for robust calcium-dependent nuclear translocation. The exposed nuclear localization signals (NLSs) are the main driving features for the nuclear translocation of dephosphorylated NFAT. The C-terminal domain of NFAT contains one of the two NLSs,¹⁹ and we hypothesized that its deletion would result in decreased nuclear translocation and thus impair constitutive transcriptional activity in uninduced cells. A previous study showed that a truncated human NFAT-c1 isoform with a deleted C-terminal transactivation domain was capable of normal nuclear translocation at elevated calcium levels in COS cells.¹⁹ We confirmed that the truncated hNFAT (hereafter referred to as “hNFAT²⁻⁵⁹²”) (Figure 2A) retained the nuclear translocation (Figure 2B) and potent transcriptional activation (Figure 2C) abilities in ionophore-stimulated HEK293T cells; however, the construct also exhibited partial nuclear translocation and undesired transcriptional activity in the uninduced state (Figure 2B,C).

When the intracellular calcium concentration is low, NFAT is rephosphorylated in the nucleus.²⁰ The conformational rearrangement, triggered by phosphorylation, exposes the nuclear export signal (NES), resulting in the translocation of NFAT to the cytosol. Nuclear export has previously been engineered into transcription factors by fusing an NES and a light-controlled protein, using illumination with blue light to induce a conformational change and expose the NES.²⁷ In our attempt to reduce the undesired constitutive activity of overexpressed hNFAT in uninduced cells, we inserted an additional HIV-1 Rev NES signal²⁸ into the truncated hNFAT²⁻⁵⁹² adjacent to the native NFAT NES, generating hNFAT^{2-592_2NES} (Figure 2D). The translocation of hNFAT^{2-592_2NES} to the nucleus triggered by ionophore-

induced calcium influx was not impaired by the additional NES; however, a large fraction of the protein remained in the cytosol even after ionophore stimulation (Figure 2E). Importantly, the constitutive activity of hNFAT^{2-592_2NES} in uninduced cells was greatly reduced compared to that of full-length hNFAT (Figure 2F). Reporter expression was efficiently activated in ionophore-treated cells, resulting in an improved 14-fold ratio between the stimulated and nonstimulated states (Figure 2F).

In another approach to alter NFAT localization, we anchored the truncated hNFAT²⁻⁵⁹² to the plasma membrane, from where it should be released in response to increased levels of intracellular calcium (Figure 2G). The plasma membrane of mammalian cells contains anionic lipids on the inner leaflet, where the accumulation of negative charges creates an electric field that attracts polycationic peptides. Examples include the farnesylated K-Ras peptide and its derivatives (K-pre and R-pre), the N-terminal myristoylated peptide K-myr, and amphiphilic helices, such as the synthetic peptide sequence KR ϕ .^{29,30} The KR ϕ , R-pre, and K-myr peptides were previously shown to localize at the plasma membrane of macrophages and be released in response to increased intracellular calcium levels.^{29,30} We first validated the localization of the KR ϕ , R-pre, and K-myr peptides in HEK293T cells by fusing them to the blue fluorescent protein (BFP) (Figure S2A). The localization of the membrane anchor-tagged fluorescent proteins was detected with confocal microscopy. As previously reported, the R-pre and KR ϕ peptides were able to anchor the fluorescent protein to the plasma membrane (Figure S2B,C); however, in contrast to previous studies, the K-myr peptide failed to exhibit efficient membrane localization²⁹ (Figure S2D). Next, the subcellular localization of BFP fused to the NFAT regulatory domain (hNFAT²⁻⁴⁰⁹:BFP) was examined (Figure S3A). As expected, tethering of this construct to either the R-pre (Figure S3B,C) or the KR ϕ peptide (Figure S3D,E) resulted in anchoring to the plasma membrane in uninduced cells (Figure S3C,E). Following ionophore stimulation, nuclear translocation was detected only for the hNFAT²⁻⁴⁰⁹:BFP:KR ϕ chimera (Figure S3E), while the R-pre peptide relocated to the endomembranes (Figure S3C), as previously shown for the K-Ras peptide and its derivatives.³¹ Next, the KR ϕ peptide was fused to the truncated hNFAT²⁻⁵⁹² variant (Figure 2H). The hNFAT²⁻⁵⁹²:KR ϕ construct was clearly translocated to the nucleus following ionophore stimulation, but it was partially retained at the plasma membrane (Figure 2I). Importantly, the construct mediated the robust, potent activation of reporter gene expression with no significant transcriptional activity in uninduced cells, resulting in a further improved 25-fold difference between the stimulated and nonstimulated states (Figure 2J).

A Western blot analysis was performed to confirm that the reduced activity of engineered NFAT variants observed in uninduced cells was not due to low protein expression. The results indicated even higher expression of all three engineered NFAT proteins (hNFAT²⁻⁵⁹², hNFAT^{2-592_2NES}, and hNFAT²⁻⁵⁹²:KR ϕ) compared to that of full-length hNFAT (Figure S4A), further confirming that the improved features are due to their engineered localization properties. Incubation of ionophore-stimulated cells with CsA verified that the calcineurin/NFAT pathway mediated the enhanced activation by the engineered proteins (Figure S4B). The constructs were additionally characterized by titration of ionophore and time-

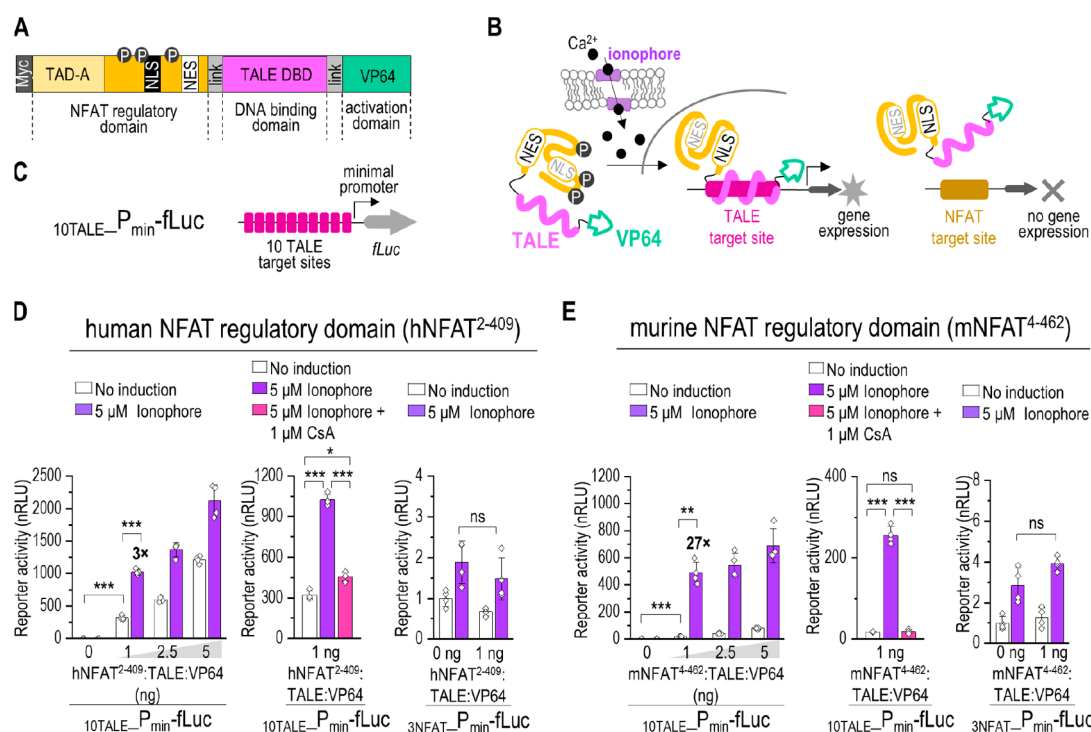


Figure 3. Replacement of the NFAT DNA-binding domain redirects transcriptional activity toward the selected promoter. (A) Schematic presentation of an engineered transcription factor composed of the NFAT regulatory domain, the TALE DNA-binding domain, and the VP64 activation domain. (B) Schematic presentation of transcriptional activation by the engineered transcription factor. Following calcium influx, the NFAT:TALE:VP64 construct is translocated to the nucleus, where it only regulates promoters containing the TALE target site, whereas promoters with the NFAT target sites are unaffected. (C) Schematic presentation of the $_{10TALE_P_{min}\text{-fLuc}}$ reporter plasmid. (D) Transcriptional activity of the engineered transcription factor containing the human NFAT regulatory domain (hNFAT²⁻⁴⁰⁹). The hNFAT²⁻⁴⁰⁹:TALE:VP64 construct strongly enhances reporter gene expression in both stimulated and nonstimulated HEK293T cells (left). The ionophore-induced increase in transcriptional activity is mediated through the calcineurin/NFAT signaling pathway (middle). The construct did not enhance the transcription of the reporter gene driven by the NFAT-regulated promoter (right). (E) Transcriptional activity of the engineered transcription factor containing the murine NFAT regulatory domain (mNFAT⁴⁻⁴⁶²). The mNFAT⁴⁻⁴⁶²:TALE:VP64 construct strongly enhances reporter gene expression in ionophore-stimulated HEK293T cells, with markedly reduced activity in the uninduced state (left). The ionophore-induced increase in transcriptional activity is mediated through the calcineurin/NFAT signaling pathway (middle). The construct did not enhance the transcription of the reporter gene driven by the NFAT-regulated promoter (right). Amounts of transfected plasmids for all luciferase experiments are listed in Table S1. One day after transfection, cells were stimulated with ionophore or both ionophore and CsA. Reporter activity was measured 6–8 h after treatment. The bars represent the mean \pm s.d.; $n = 4$ biologically independent cell cultures. Statistical analyses and the corresponding p -values are listed in Table S2.

lapse measurements of transcriptional activity (Figure S4C,D). All engineered variants reached peak activity even at the lowest concentration of ionophore tested (1 μ M) (Figure S4C) and after 6 h of stimulation (Figure S4D). Among the tested approaches to engineer an optimal NFAT variant for use in synthetic biological circuits, the hNFAT²⁻⁵⁹²:KR ϕ protein exhibited the lowest background activity in uninduced cells. Meanwhile, the construct retained the ability to potently activate transcription in response to increased intracellular calcium concentrations. These results suggest that tagging NFAT-based constructs with the KR ϕ membrane anchor peptide is a suitable strategy for further implementation in more complex synthetic circuits.

Rewiring NFAT Signaling toward Selected DNA Targets. For the optimal performance of engineered biological circuits, it is crucial that they function independently of the host cell's endogenous processes. In addition to activating an exogenously introduced transgene, the overexpressed hNFAT proteins may also mediate the undesired regulation of autologous genes. To engineer a calcium-responsive transcription factor that does not interfere with the endogenous NFAT-regulated genes, we modified the engineered

hNFAT²⁻⁵⁹² protein by replacing its DNA-binding domain with a synthetic TALE DNA-binding domain and the VP64 activation domain (Figure 3A). This engineered transcription factor should only bind to the synthetic TALE target site and not to NFAT target sites, eliminating the undesired off-target activity (Figure 3B). HEK293T cells were cotransfected with the plasmid encoding the synthetic hNFAT²⁻⁴⁰⁹:TALE:VP64 transcription factor and a reporter plasmid with 10 repeats of the TALE binding site upstream of a minimal promoter ($_{10TALE_P_{min}\text{-fLuc}}$) (Figure 3C). The construct initiated strong ionophore-triggered transcription from the synthetic promoter that was mediated through the calcineurin/NFAT pathway, as confirmed by incubation with a combination of ionophore and CsA (Figure 3D). Importantly, the construct was unable to activate transcription from an NFAT-driven promoter (Figure 3D), demonstrating that NFAT signaling can be rewired toward the selected target promoter, orthogonal to endogenous NFAT-regulated genes. However, as expected based on the NFAT overexpression results (Figure 1E), the hNFAT²⁻⁴⁰⁹:TALE:VP64 chimera also exhibited substantial transcriptional activity in uninduced cells (Figure 3D), despite

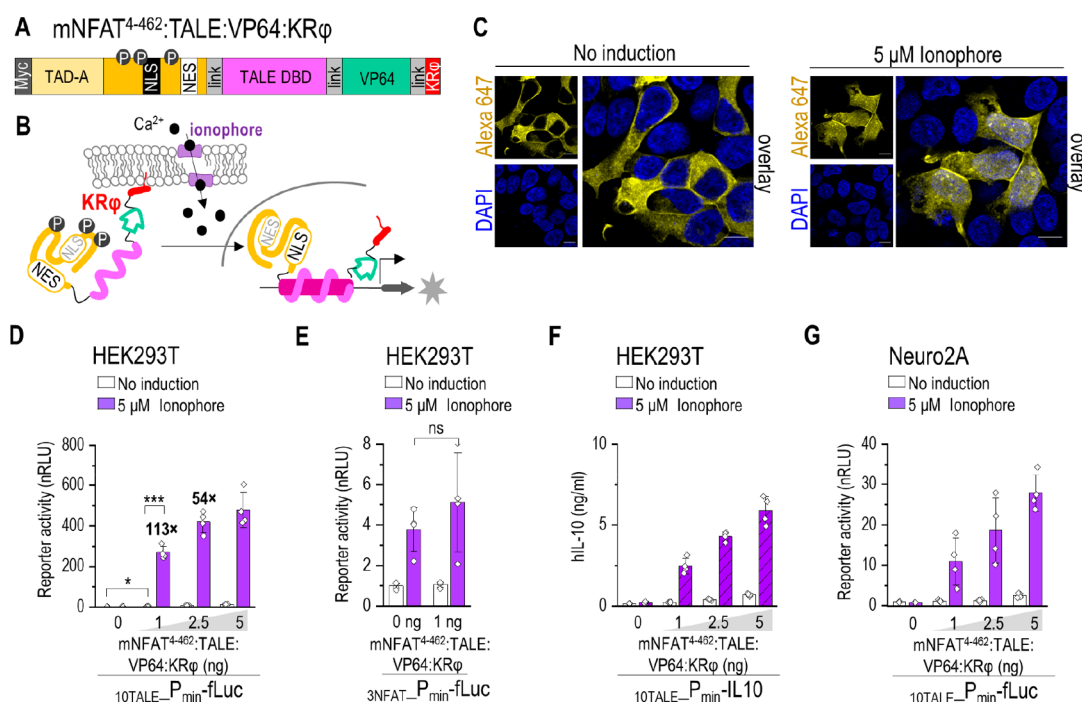


Figure 4. An engineered NFAT-based transcription factor enables highly potent calcium-mediated signaling. (A) Schematic presentation of the mNFAT⁴⁻⁴⁶²:TALE:VP64:KR ϕ construct. (B) Schematic presentation of transcriptional activation by the mNFAT⁴⁻⁴⁶²:TALE:VP64:KR ϕ transcription factor. In the absence of calcium influx, the KR ϕ peptide anchors the construct to the plasma membrane. Following ionophore stimulation and increased cytosolic calcium levels, the peptide is released, and the transcription factor is translocated to the nucleus, where it regulates transcription from the corresponding promoter. (C) Confocal microscopy images of HEK293T cells transfected with 100 ng of plasmid encoding mNFAT⁴⁻⁴⁶²:TALE:VP64:KR ϕ . The images were acquired 1 day after transfection following 3 h of cultivation with or without ionophore and immunostaining with DAPI, anti-Myc tag primary antibodies, and Alexa 647-conjugated secondary antibodies. The scale bars represent 10 μ m. (D) The mNFAT⁴⁻⁴⁶²:TALE:VP64:KR ϕ construct exhibits strongly reduced constitutive activity in nonstimulated HEK293T cells, with a 113-fold change in luciferase reporter expression following stimulation with ionophore. (E) The mNFAT⁴⁻⁴⁶²:TALE:VP64:KR ϕ construct did not enhance transcription of the reporter gene driven by the NFAT-regulated promoter in HEK293T cells. (F) mNFAT⁴⁻⁴⁶²:TALE:VP64:KR ϕ -mediated activation of the expression of a transgenic human interleukin 10 in HEK293T cells. (G) mNFAT⁴⁻⁴⁶²:TALE:VP64:KR ϕ -mediated activation of luciferase reporter expression in the mouse neuroblastoma Neuro2A cell line. Amounts of transfected plasmids for all luciferase and ELISA experiments are listed in Table S1 and S3. One day after transfection, cells were stimulated with ionophore. ELISA sample collection and reporter activity measurements were performed 6–8 h after treatment. The bars represent the mean \pm s.d.; $n = 4$ biologically independent cell cultures. Statistical analyses and the corresponding p -values are listed in Table S2.

its apparent cytosolic localization in the absence of ionophore (Figure S5A).

For our aim of achieving potent transcriptional activity following calcium influx and minimal activity in uninduced cells, we set out to test NFAT orthologues from other organisms. NFAT orthologues may have different biochemical properties than their human counterpart, potentially making them more suitable for use in engineered biological circuits. Recently, a calcium-dependent dCas9-VP64 transcriptional activator, which exhibited low activity in uninduced HeLa cells, was engineered by fusion to the murine NFAT regulatory domain (mNFAT⁴⁻⁴⁶²).²¹ We replaced the human hNFAT regulatory domain with its murine homologue, generating mNFAT⁴⁻⁴⁶²:TALE:VP64. The construct supported highly potent reporter gene expression in ionophore-stimulated cells, which was mediated through the calcineurin/NFAT pathway, and did not activate transcription from the NFAT-driven promoter (Figure 3E). Similar to the construct containing the human NFAT regulatory domain, ionophore stimulation induced cytosolic localization followed by robust nuclear translocation, as detected with confocal microscopy (Figure S5B). Activity in uninduced cells was significant; nevertheless, it was strikingly lower than that with the construct containing the human NFAT regulatory domain, reaching a 27-fold

difference between the induced and uninduced states (Figure 3E).

To further reduce the undesired transcriptional activity in uninduced cells, the KR ϕ anchor peptide was appended to the C-terminus of both NFAT:TALE:VP64 chimeras (Figure 4A, Figure S6A). Both constructs displayed similar localization at the plasma membrane and in the cytosol, followed by ionophore-triggered translocation to the nucleus (Figure 4C, Figure S6B). The construct containing the human NFAT regulatory domain (hNFAT²⁻⁴⁰⁹:TALE:VP64:KR ϕ) efficiently activated transcription of the luciferase reporter with strongly decreased activity in uninduced cells and an improved 18-fold difference between the stimulated and nonstimulated states (Figure S6C). Additionally, as a demonstration of the potential therapeutic applications of the NFAT-based circuit, the construct activated the expression of a transgenic human anti-inflammatory cytokine interleukin 10 (hIL-10) (Figure S6D). The remaining undesired activation may be due to signal amplification, as the reporter plasmid contains 10 copies of the TALE target site in contrast to the 3NFAT_{min}-fLuc reporter plasmid containing only three copies of the NFAT target site. No transcriptional activation was observed in uninduced cells when the synthetic promoter contained a single copy of the TALE target site (Figure S6E,F).

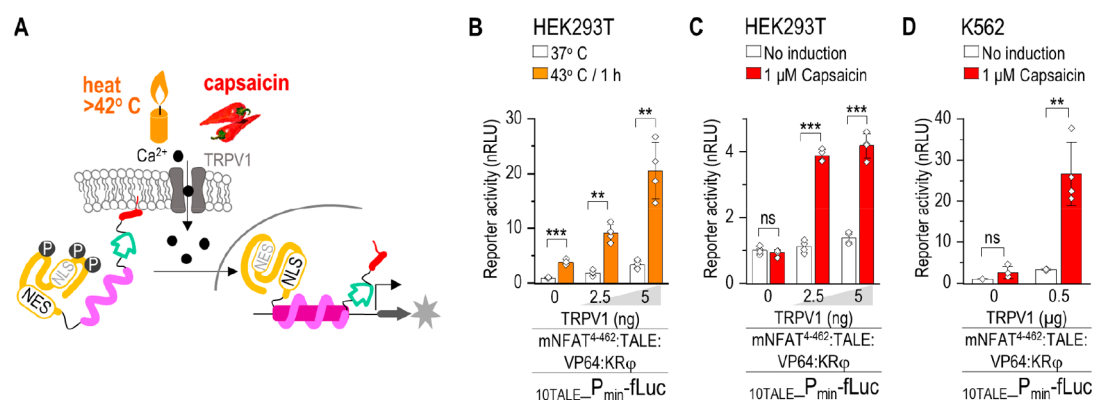


Figure 5. Temperature- and capsaicin-triggered activation of the engineered NFAT-based signaling pathway. (A) Schematic presentation of the external stimuli-controlled pathway. Stimulation of TRPV1 by heat or capsaicin induces the influx of calcium ions and thus the release, translocation, and transcriptional activation by the mNFAT⁴⁻⁴⁶²:TALE:VP64:KR ϕ transcription factor. (B) Incubation at 43 °C significantly activates transcription of the reporter gene in HEK293T cells, with enhanced activity upon cotransfection of the TRPV1-encoding plasmid. (C) Capsaicin significantly activates transcription of the reporter gene in TRPV1-expressing HEK293T cells. (D) Capsaicin significantly activates transcription of the reporter gene in TRPV1-expressing K562 cells. Amounts of transfected and electroporated plasmids for all luciferase experiments are listed in Table S1 and S4. One day after transfection, cells were incubated at 43 °C for 1 h or stimulated with capsaicin. Reporter activity was measured 6–8 h after treatment. The bars represent the mean \pm s.d.; $n = 4$ biologically independent cell cultures. Statistical analyses and the corresponding p -values are listed in Table S2.

Nevertheless, while reporter gene expression in ionophore-stimulated cells was significantly elevated, it was 2 orders of magnitude weaker than that of the reporter plasmid with 10 copies of the target site (Figure S6C).

The mNFAT⁴⁻⁴⁶²:TALE:VP64:KR ϕ construct exhibited low transcriptional activity in uninduced cells, and it was potently activated following ionophore addition, with over 100-fold difference between the stimulated and nonstimulated states (Figure 4D). As expected, the construct did not activate transcription from the NFAT-driven promoter (Figure 4E). Additionally, mNFAT⁴⁻⁴⁶²:TALE:VP64:KR ϕ activated the expression of the hIL-10 transgene in HEK293T cells (Figure 4F) and luciferase reporter gene expression in the Neuro2A mouse neuroblastoma cell line (Figure 4G), further demonstrating its versatility. Among the tested NFAT:TALE chimeras, the mNFAT⁴⁻⁴⁶²:TALE:VP64:KR ϕ construct clearly exhibited the best properties for use in synthetic genetic circuits that exploit calcium signaling.

Activation of the Engineered NFAT-Based Signaling Pathway by Physical and Chemical Stimuli. To establish the utility of the engineered NFAT:TALE chimeras for responding to diverse extracellular signals, the expression of an exogenously introduced gene was coupled with a calcium-selective ion channel. Light-dependent control of calcium influx has previously been engineered into mammalian cells by overexpressing ORAI/STIM calcium selective channels.^{16,32,33} To expand the selection of stimuli for the external control of intracellular calcium levels, other calcium-transducing receptors need to be explored. The transient receptor potential (TRP) channel TRPV1 belongs to a group of plasma membrane ion channels that sense various hot and cool temperature thresholds.^{34,35} The TRPV1-driven influx of calcium ions is triggered by temperatures above 42 °C or the presence of small molecules such as capsaicin, an active component of chili peppers.³³ Here, human TRPV1-induced intracellular calcium-influx was used to promote the translocation of the mNFAT⁴⁻⁴⁶²:TALE:VP64:KR ϕ transcription factor and activate gene expression in a temperature- or capsaicin-dependent manner (Figure 5A). The synthetic circuit responded to a temperature of 43 °C (Figure 5B), as

demonstrated by the activation of firefly luciferase reporter gene expression in HEK293T cells. The increase in temperature to 43 °C activated reporter gene expression even in cells without the cotransfected TRPV1 ion channel, suggesting that the endogenous HEK293T thermal sensors³⁵⁻³⁷ may have activated the NFAT-based gene circuit (Figure 5B). In parallel, capsaicin significantly activated gene expression only in HEK293T and K562 cells that were cotransfected with the TRPV1 channel (Figure 5C,D). These results clearly demonstrate that the NFAT-based transcription factors engineered in this study can be controlled *via* selected, physiologically relevant physicochemical signals through the introduction of calcium-selective receptors.

CONCLUSIONS

We report a synthetic, calcium-dependent, NFAT-based genetic circuit that regulates transcription in response to external signals that trigger increases in cytosolic calcium concentrations. Because the endogenous NFAT of host cells exhibited a weak response, we overexpressed the human NFAT-c1 isoform (hNFAT) in HEK293T cells, which strongly enhanced the transcriptional activation of a reporter gene. The problem of partial nuclear translocation and NFAT activity in uninduced cells was solved by engineering NFAT variants with enforced localization. Fusion of hNFAT to the plasma membrane anchor peptide KR ϕ was found to be the most favorable strategy and resulted in minimal apparent transcriptional activity in uninduced cells and up to a 25-fold increase in the activation of reporter expression following ionophore treatment. Moreover, confocal microscopy results demonstrated the incomplete release of the peptides from the plasma membrane, suggesting that the system could be even further improved by engineering the peptide sequence. To eliminate the regulation of endogenous NFAT promoters by the engineered NFAT variants, the NFAT DNA-binding domain was replaced with a designed TALE DNA-binding domain and the VP64 activation domain. This yielded potent transcriptional activators that were dependent on the intracellular calcium concentration, demonstrating the modularity of

NFAT-based synthetic circuits. The designable NFAT-TALE transcription factors can be used for calcium-dependent targeting and regulation of endogenous gene expression, as the TALE DNA-binding domains can be designed to bind any selected sequence. In principle, the TALE DNA-binding domain can be exchanged with the CRISPR/dCas9 catalytically inactive nuclease,²¹ zinc-finger DNA-binding domains, or any other effector domain with a function that relies on nuclear localization. The versatility of the engineered NFAT-based transcription factors was demonstrated by their functionality in different mammalian cell types (the human embryonic kidney cell line HEK293T, the mouse neuroblastoma cell line Neuro2A, and the human granulocyte cell line K562). The engineered transcription factors also induced the transcription of the transgenic anti-inflammatory cytokine hIL-10 in response to a calcium influx, suggesting its potential use in therapeutic applications. We coupled the gene circuit to the TRPV1 ion channel, resulting in capsaicin- and temperature-dependent transcriptional activation. In place of TRPV1, the circuit could be coupled to other physicochemically inducible calcium ion-selective membrane receptors, such as different G-protein coupled receptors or ion channels. The engineered NFAT-based transcription factors presented in this study represent valuable tools for use in synthetic biology and are applicable in a wide range of therapeutic and diagnostic applications, and they will be useful tools for investigating natural processes.

MATERIALS AND METHODS

Cloning and Plasmid Construction. All plasmids were constructed using the Gibson assembly method,³⁸ and their amino acid or nucleotide sequences are listed in Tables S5 and S6.

Cell Culture. The embryonic kidney HEK293T cell line (ATCC) was cultured in Dulbecco's modified Eagle's medium (DMEM; Invitrogen) supplemented with 10% fetal bovine serum (Gibco) at 37 °C in a 5% CO₂ environment. The mouse neuroblastoma Neuro2A cell line (ATCC) was cultured in OptiMEM (Invitrogen) supplemented with 10% fetal bovine serum (Gibco) at 37 °C in a 5% CO₂ environment. The human immortalized myelogenous leukemia K562 cell line (ATCC) was cultured in RPMI (Invitrogen) supplemented with 10% fetal bovine serum (Gibco) at 37 °C in a 5% CO₂ environment.

Transfection, Electroporation, and Stimulation. For dual luciferase assays and ELISAs, 2×10^4 HEK293T cells or 3×10^4 Neuro2A cells were seeded per well in 96-well plates (Corning). For confocal microscopy experiments, 3×10^4 HEK293T cells were seeded per well in an 8-well chamber slide (Ibidi). For Western blot experiments, 5×10^5 HEK293T cells were seeded per well in 6-well plates (Corning). At 50–70% confluence, HEK293T cells were transfected with a mixture of DNA and polyethylenimine (PEI, linear, Mw 25000; Polysciences, catalog no. 23966). Per 500 ng DNA, 6 μ L of PEI stock solution (0.324 mg mL⁻¹, pH 7.5) was used. Neuro2A cells were transfected at 80–90% confluence using a mixture of DNA and Lipofectamine LTX (Thermo Fisher Scientific) following the manufacturer's instructions. K562 cells were electroporated with the Gene Pulser electroporation system (Bio Rad) in 0.4 cm cuvettes at 350 V, 500 μ F. A total of 20 μ g of DNA was used to electroporate 3×10^5 cells for each sample. After electroporation, the cells were resuspended in 2 mL of fresh medium and seeded into 96-well plates at 100

μ L per well. Twenty-four h after transfection or electroporation, the culture medium was replaced with fresh medium, and cells were stimulated with the indicated concentration of ionophore (calcium ionophore A23187, Sigma-Aldrich), cyclosporine A (BioVision), or capsaicin (Sigma-Aldrich) for the indicated times. Calcium ionophore A23187 was prepared as a 10 mM stock solution in DMSO, capsaicin as a 100 mM stock solution in ethanol, and cyclosporine A as a 25 mM stock solution in DMSO. "No induction" means incubation with the solvent used for the stock solution in the experiment. In experiments where cyclosporine A was used in combination with ionophore, cells were preincubated with 1 μ M cyclosporine A for 30 min before stimulation with ionophore. For temperature stimulation experiments, cells were incubated at the indicated temperature for 2 h and kept at 37 °C for 4 h before lysis. The amounts of transfected plasmids are indicated in the figures and figure captions or presented in Tables S1, S3, and S4. The phRL-TK plasmid (Promega), encoding the *Renilla* luciferase, was used as a transfection efficiency control in luciferase experiments. The empty pcDNA3 plasmid (Invitrogen) was used to equalize the total DNA amounts over different experimental conditions.

Dual Luciferase Assays. Cells were lysed at the indicated time points using 25 μ L of 1 \times Passive lysis buffer (Promega) per well. Firefly luciferase (fLuc) and *Renilla* luciferase (rLuc) activities were measured using the dual luciferase assay (Promega) on an Orion II microplate reader (Berthold Technologies). Relative luciferase units (RLUs) were calculated by normalizing fLuc to the constitutive rLuc in each sample. Normalized RLU (nRLU) values were calculated by normalizing the RLU values of each sample to the average RLU value of the nonstimulated reporter only samples within the same experiment. For the experiments in Figure 5, nRLU values were calculated by normalizing the RLU values of each sample to the average RLU value of the nonstimulated cells transfected with 0 ng of the TRPV1-encoding plasmid. Fold activation (depicted above the bars) was calculated as the ratio between the average nRLUs of stimulated and nonstimulated samples.

Immunostaining and Confocal Microscopy. For immunofluorescent analysis of protein localization, cells were fixed with 4% formaldehyde (Histofix, Roth) and permeabilized with 0.1% Triton X-100 (Thermo Scientific) 1 day after transfection. The cells were stained with anti-Myc tag rabbit polyclonal primary antibodies (C3956, Sigma-Aldrich) at a dilution of 1:100 and then incubated with Alexa Fluor 647-conjugated goat antirabbit IgG secondary antibodies at a dilution of 1:2000 (A-21246, Invitrogen); 300 nM DAPI (Invitrogen) was used as a nuclear stain. After immunostaining, the cells were washed with PBS and stained with DAPI for 5 min. For analyses of fluorescent protein-expressing cells, live cells were imaged 1 day after transfection. During microscopy, the cells were kept in a chamber at 37 °C. To maintain the physiological pH, 10 mM HEPES pH 7.4 (from 1 M stock solution) was added to the media. Microscopic images were obtained using a Leica TCS SP5 inverted laser-scanning microscope on a Leica DMI 6000 CS module equipped with an HCX Plane-Apochromat lambda blue 63 \times objective, numerical aperture 1.4 (Leica Microsystems). A 50 mW 405 nm diode laser was used for BFP and DAPI excitation (emission between 420 and 460 nm), and a 10 mW 633 nm HeNe laser was used for Alexa Fluor 647 excitation (emission between 650 and 690 nm). To evaluate the nuclear

translocation of engineered calcium-dependent constructs, BFP-fused constructs were transfected into HEK293T cells and then incubated for 4 h either in medium (nonstimulated) or with 5 μ M ionophore (calcium ionophore A23187, Sigma-Aldrich). Leica LAS AF software was used for acquisition, and ImageJ software (National Institute of Mental Health, Bethesda, USA) was used for image processing.

Immunoblotting. Two days after transfection, the cells were washed with 1 mL of PBS and lysed in 100 μ L of 1 \times Passive lysis buffer (Promega). The protein concentration in each sample was determined with the bicinchoninic acid (BCA) assay. Sample dilutions (1:15 in water, 30 μ L) and BSA standard were mixed with 200 μ L of the BCA reagent (CuSO₄ diluted 1:50 in bicinchoninic acid) and incubated at 37 °C for 30 min. Absorbance at 562 nm was measured on a Synergy Mx automated microplate reader (BioTek) using Gen5 software. Measurements were corrected by subtraction of the absorbance of the blank sample (water) at 562 nm. Samples (75 μ g of total protein per sample) were separated by SDS-PAGE (200 V, 10% polyacrylamide gel) and transferred to a Hybond ECL nitrocellulose membrane (GE Healthcare) at 350 mA. The membrane was incubated with anti-Myc tag primary antibodies (1:1000, rabbit anti-c-Myc IgG; Sigma-Aldrich, C3956) and with secondary antibodies (1:4000, goat antirabbit IgG-HRP; Invitrogen, 65–6120). Membrane blocking, antibody binding, and membrane washing were performed with an iBind Flex Western Device (Thermo Fisher) according to the manufacturer's protocol. The immunoblots were visualized in a G-box analyzer (Syngene) after they were developed using the Pico Sensitivity substrate (Thermo Fisher Scientific). ImageJ software (National Institute of Mental Health, Bethesda, USA) was used for image processing and densitometric analysis.

ELISA. Supernatants were collected 6 h after cell stimulation and stored at –20 °C overnight before ELISA for hIL-10 (IL-10 Human Uncoated ELISA kit, 88–7106–77, Thermo Scientific) was performed following the manufacturer's instructions, using appropriate dilutions. Absorbance was measured on a Synergy Mx automated microplate reader (BioTek) at 450 and 630 nm using Gen5 software. Absorbance at 630 nm was used for correction and was subtracted from the absorbance at 450 nm.

Statistical Analysis. Data are presented as the mean \pm s.d. of 4 biological replicates within the same experiment. Graphs were prepared with Origin 8.1 software, and GraphPad Prism 6 was used for statistical purposes. For analysis of activity in uninduced cells transfected with increasing amounts of the NFAT variant-encoding plasmid, one-way ANOVA with Dunnett's *post hoc* analysis was used. The mean of each treatment (different NFAT variant-encoding plasmid amounts) was compared to the mean of the control treatment (0 ng of the NFAT variant-encoding plasmid). For analysis of experiments in which cells were treated with cyclosporine A and/or ionophore, one-way ANOVA with Tukey's *post hoc* analysis was used. The mean of each treatment was compared to the mean of every other treatment. For analysis of treated and nontreated cells within the same experimental condition (the same NFAT variant-encoding plasmid amount), paired, two-tailed Student's *t* tests were used. The details of the statistical tests along with the *p*-values for each figure panel are listed in Table S2.

■ ASSOCIATED CONTENT

SI Supporting Information

The Supporting Information is available free of charge at <https://pubs.acs.org/doi/10.1021/acssynbio.0c00133>.

Transcriptional activation of a transiently introduced reporter by the native NFAT in HEK293T cells (Figure S1); Localization of a fluorescent protein fused to membrane anchoring peptides in HEK293T cells (Figure S2); Localization of the NFAT regulatory domain and a fluorescent protein fused to membrane anchoring peptides in HEK293T cells (Figure S3); Characterization of the expression and transcriptional activation by the engineered NFAT variants in HEK293T cells (Figure S4); Subcellular localization of the NFAT regulatory domain fused to the TALE DNA-binding domain and the VP64 activation domain (Figure S5); The KR ϕ anchor peptide reduces the undesired activation by the hNFAT^{2–409}:TALE:VP64 construct (Figure S6); Amounts of transfected plasmids for HEK293T cells in each well of a 96-well plate (Table S1); Statistical analyses data (Table S2); Amounts of transfected plasmids for Neuro2A cells in each well of a 96-well plate (Table S3); Amounts of electroporated plasmids for K562 cells in each electroporation sample (Table S4); Amino acid sequences of the proteins used in this study (Table S5); Nucleotide sequences of the promoters and target sites used in this study (Table S6) (PDF)

■ AUTHOR INFORMATION

Corresponding Authors

Roman Jerala – Department of Synthetic Biology and Immunology, National Institute of Chemistry, SI-1001 Ljubljana, Slovenia; EN-FIST Centre of Excellence, SI-1000 Ljubljana, Slovenia; Email: roman.jerala@ki.si

Mojca Benčina – Department of Synthetic Biology and Immunology, National Institute of Chemistry, SI-1001 Ljubljana, Slovenia; EN-FIST Centre of Excellence, SI-1000 Ljubljana, Slovenia; orcid.org/0000-0002-3644-9948; Email: mojca.bencina@ki.si

Authors

Maja Meško – Department of Synthetic Biology and Immunology, National Institute of Chemistry, SI-1001 Ljubljana, Slovenia; Interfaculty Doctoral Study of Biomedicine, University of Ljubljana, SI-1000 Ljubljana, Slovenia

Tina Lebar – Department of Synthetic Biology and Immunology, National Institute of Chemistry, SI-1001 Ljubljana, Slovenia

Petra Dekleva – Department of Synthetic Biology and Immunology, National Institute of Chemistry, SI-1001 Ljubljana, Slovenia

Complete contact information is available at:

<https://pubs.acs.org/doi/10.1021/acssynbio.0c00133>

Author Contributions

^{||}MM and TL have shared first authorship.

Author Contributions

MM, TL, and PD prepared the plasmid constructs and performed the experiments. TL, MM, and MB wrote the manuscript. MB processed the data and prepared the figures. MB and RJ conceived the study. All authors read the

manuscript, discussed the results, and commented on the manuscript before submission.

Notes

The authors declare no competing financial interest.

ACKNOWLEDGMENTS

We thank Irena Škraba for isolation of the plasmids and Anja Perčič for help with the luciferase measurements. Work on this project was financed by programs and projects from the Slovenian Research Agency (P4-0176, J4-1779, and J3-9268), European Commission Horizon 2020 Coordination and Support Action, project Bioroboost (H2020-NMBP-BIO-CSA-2018, grant ID 820699), European Research Area M-ERA.NET project MediSurf (grant ID 3193), ICGEB project (CRP/SVN18-01, Contract CRP/19/019), and COST actions (CM-1306 and CM-1304).

ABBREVIATIONS

BCA, bichinchoninic acid; BFP, blue fluorescent protein; BSA, bovine serum albumin; CsA, cyclosporine A; CRISPR, clustered regularly interspaced short palindromic repeats; DAPI, 4',6-diamidino-2-phenylindole; fLuc, firefly luciferase; IL-10, interleukin 10; NES, nuclear export signal; NFAT, nuclear factor of activated T-cells; NLS, nuclear localization signal; rLuc, *Renilla* luciferase; TALE, transcription activator-like effectors; TRPV1, transient receptor potential channel.

REFERENCES

- (1) Bashor, C. J., Patel, N., Choubey, S., Beyzavi, A., Kondev, J., Collins, J. J., and Khalil, A. S. (2019) Complex Signal Processing in Synthetic Gene Circuits Using Cooperative Regulatory Assemblies. *Science* 364 (6440), 593–597.
- (2) Weber, W., Rimann, M., Spielmann, M., Keller, B., Baba, M. D.-E., Aubel, D., Weber, C. C., and Fussenegger, M. (2004) Gas-Inducible Transgene Expression in Mammalian Cells and Mice. *Nat. Biotechnol.* 22 (11), 1440–1444.
- (3) Stanley, S. A., Gagner, J. E., Damanpour, S., Yoshida, M., Dordick, J. S., and Friedman, J. M. (2012) Radio-Wave Heating of Iron Oxide Nanoparticles Can Regulate Plasma Glucose in Mice. *Science (Washington, DC, U. S.)* 336 (6081), 604–608.
- (4) Bai, P., Liu, Y., Xue, S., Hamri, G. C.-E., Saxena, P., Ye, H., Xie, M., and Fussenegger, M. (2019) A Fully Human Transgene Switch to Regulate Therapeutic Protein Production by Cooling Sensation. *Nat. Med.* 25 (8), 1266–1273.
- (5) Deans, T. L., Cantor, C. R., and Collins, J. J. (2007) A Tunable Genetic Switch Based on RNAi and Repressor Proteins for Regulating Gene Expression in Mammalian Cells. *Cell* 130 (2), 363–372.
- (6) Zhang, F., Cong, L., Lodato, S., Kosuri, S., Church, G. M., and Arlotta, P. (2011) Efficient Construction of Sequence-Specific TAL Effectors for Modulating Mammalian Transcription. *Nat. Biotechnol.* 29 (2), 149–153.
- (7) Cong, L., Zhou, R., Kuo, Y.-C., Cunniff, M., and Zhang, F. (2012) Comprehensive Interrogation of Natural TALE DNA-Binding Modules and Transcriptional Repressor Domains. *Nat. Commun.* 3, 968.
- (8) Gaber, R., Lebar, T., Majerle, A., Ster, B., Dobnikar, A., Benčina, M., and Jerala, R. (2014) Designable DNA-Binding Domains Enable Construction of Logic Circuits in Mammalian Cells. *Nat. Chem. Biol.* 10 (3), 203–208.
- (9) Lebar, T., Bezeljak, U., Golob, A., Jerala, M., Kadunc, L., Pirš, B., Stražar, M., Vučko, D., Zupančič, U., Benčina, M., et al. (2014) A Bistable Genetic Switch Based on Designable DNA-Binding Domains. *Nat. Commun.* 5, 5007.
- (10) Lebar, T., and Jerala, R. (2016) Benchmarking of TALE- and CRISPR/DCas9-Based Transcriptional Regulators in Mammalian

Cells for the Construction of Synthetic Genetic Circuits. *ACS Synth. Biol.* 5 (10), 1050–1058.

- (11) Jinek, M., Chylinski, K., Fonfara, I., Hauer, M., Doudna, J. A., and Charpentier, E. (2012) A Programmable Dual-RNA-Guided DNA Endonuclease in Adaptive Bacterial Immunity. *Science (Washington, DC, U. S.)* 337 (6096), 816–821.

- (12) Qi, L. S., Larson, M. H., Gilbert, L. A., Doudna, J. A., Weissman, J. S., Arkin, A. P., and Lim, W. A. (2013) Repurposing CRISPR as an RNA-Guided Platform for Sequence-Specific Control of Gene Expression. *Cell* 152 (5), 1173–1183.

- (13) Lonžarić, J., Lebar, T., Majerle, A., Mancek-Keber, M., and Jerala, R. (2016) Locked and Proteolysis-Based Transcription Activator-like Effector (TALE) Regulation. *Nucleic Acids Res.* 44 (3), 1471–1481.

- (14) Polstein, L. R., and Gersbach, C. A. (2015) A Light-Inducible CRISPR-Cas9 System for Control of Endogenous Gene Activation. *Nat. Chem. Biol.* 11 (3), 198–200.

- (15) Lebar, T., Lainšček, D., Merljak, E., Aupič, J., and Jerala, R. (2020) A Tunable Orthogonal Coiled-Coil Interaction Toolbox for Engineering Mammalian Cells. *Nat. Chem. Biol.* 16, 513.

- (16) Kyung, T., Lee, S., Kim, J. E., Cho, T., Park, H., Jeong, Y.-M., Kim, D., Shin, A., Kim, S., Baek, J., et al. (2015) Optogenetic Control of Endogenous Ca²⁺ Channels in Vivo. *Nat. Biotechnol.* 33 (10), 1092–1096.

- (17) Ma, G., Wen, S., He, L., Huang, Y., Wang, Y., and Zhou, Y. (2017) Optogenetic Toolkit for Precise Control of Calcium Signaling. *Cell Calcium* 64, 36.

- (18) Lee, D., Hyun, J. H., Jung, K., Hannan, P., and Kwon, H.-B. (2017) A Calcium- and Light-Gated Switch to Induce Gene Expression in Activated Neurons. *Nat. Biotechnol.* 35 (9), 858–863.

- (19) Beals, C. R., Clipstone, N. A., Ho, S. N., and Crabtree, G. R. (1997) Nuclear Localization of NF-ATc by a Calcineurin-Dependent, Cyclosporin-Sensitive Intramolecular Interaction. *Genes Dev.* 11 (7), 824–834.

- (20) Hogan, P. G., Chen, L., Nardone, J., and Rao, A. (2003) Transcriptional Regulation by Calcium, Calcineurin, and NFAT. *Genes Dev.* 17 (18), 2205–2232.

- (21) Nguyen, N. T., He, L., Martinez-Moczygemba, M., Huang, Y., and Zhou, Y. (2018) Rewiring Calcium Signaling for Precise Transcriptional Reprogramming. *ACS Synth. Biol.* 7 (3), 814–821.

- (22) Liu, Y., Charpin-El Hamri, G., Ye, H., and Fussenegger, M. (2018) A Synthetic Free Fatty Acid-Regulated Transgene Switch in Mammalian Cells and Mice. *Nucleic Acids Res.* 46 (18), 9864–9874.

- (23) Pan, Y., Yoon, S., Sun, J., Huang, Z., Lee, C., Allen, M., Wu, Y., Chang, Y.-J., Sadelain, M., Shung, K. K., et al. (2018) Mechanogenetics for the Remote and Noninvasive Control of Cancer Immunotherapy. *Proc. Natl. Acad. Sci. U. S. A.* 115 (5), 992–997.

- (24) Tastanova, A., Folcher, M., Müller, M., Camenisch, G., Ponti, A., Horn, T., Tikhomirova, M. S., and Fussenegger, M. (2018) Synthetic Biology-Based Cellular Biomedical Tattoo for Detection of Hypercalcemia Associated with Cancer. *Sci. Transl. Med.* 10 (437), eaap8562.

- (25) Li, Q., Shakyia, A., Guo, X., Zhang, H., Tantin, D., Jensen, P. E., and Chen, X. (2012) Constitutive Nuclear Localization of NFAT in Foxp3⁺ Regulatory T Cells Independent of Calcineurin Activity. *J. Immunol.* 188 (9), 4268–4277.

- (26) Jia, Y.-Y., Lu, J., Huang, Y., Liu, G., Gao, P., Wan, Y.-Z., Zhang, R., Zhang, Z.-Q., Yang, R.-F., Tang, X., et al. (2014) The Involvement of NFAT Transcriptional Activity Suppression in SIRT1-Mediated Inhibition of COX-2 Expression Induced by PMA/Ionomycin. *PLoS One* 9 (5), e97999.

- (27) Niopek, D., Benzinger, D., Roensch, J., Draebing, T., Wehler, P., Eils, R., and Di Ventura, B. (2014) Engineering Light-Inducible Nuclear Localization Signals for Precise Spatiotemporal Control of Protein Dynamics in Living Cells. *Nat. Commun.* 5, 4404.

- (28) Behrens, R. T., Aligeti, M., Pocock, G. M., Higgins, C. A., and Sherer, N. M. (2017) Nuclear Export Signal Masking Regulates HIV-1 Rev Trafficking and Viral RNA Nuclear Export. *J. Virol.* DOI: 10.1128/JVI.02107-16.

- (29) Yeung, T., Terebiznik, M., Yu, L., Silvius, J., Abidi, W. M., Philips, M., Levine, T., Kapus, A., and Grinstein, S. (2006) Receptor Activation Alters Inner Surface Potential During Phagocytosis. *Science (Washington, DC, U. S.)* 313 (5785), 347–351.
- (30) Yeung, T., Gilbert, G. E., Shi, J., Silvius, J., Kapus, A., and Grinstein, S. (2008) Membrane Phosphatidylserine Regulates Surface Charge and Protein Localization. *Science (Washington, DC, U. S.)* 319 (5860), 210–213.
- (31) Yeung, T., Heit, B., Dubuisson, J.-F., Fairn, G. D., Chiu, B., Inman, R., Kapus, A., Swanson, M., and Grinstein, S. (2009) Contribution of Phosphatidylserine to Membrane Surface Charge and Protein Targeting during Phagosome Maturation. *J. Cell Biol.* 185 (5), 917–928.
- (32) He, L., Zhang, Y., Ma, G., Tan, P., Li, Z., Zang, S., Wu, X., Jing, J., Fang, S., and Zhou, L. (2015) Near-Infrared Photoactivatable Control of Ca²⁺ Signaling and Optogenetic Immunomodulation. *eLife*, DOI: 10.7554/eLife.10024.
- (33) Ishii, T., Sato, K., Kakumoto, T., Miura, S., Touhara, K., Takeuchi, S., and Nakata, T. (2015) Light Generation of Intracellular Ca²⁺ Signals by a Genetically Encoded Protein BACCS. *Nat. Commun.* 6, 8021.
- (34) Caterina, M. J., Schumacher, M. A., Tominaga, M., Rosen, T. A., Levine, J. D., and Julius, D. (1997) The Capsaicin Receptor: A Heat-Activated Ion Channel in the Pain Pathway. *Nature* 389 (6653), 816–824.
- (35) Vriens, J., Nilius, B., and Voets, T. (2014) Peripheral Thermosensation in Mammals. *Nat. Rev. Neurosci.* 15 (9), 573–589.
- (36) Luo, L., Wang, Y., Li, B., Xu, L., Kamau, P. M., Zheng, J., Yang, F., Yang, S., and Lai, R. (2019) Molecular Basis for Heat Desensitization of TRPV1 Ion Channels. *Nat. Commun.* 10 (1), 2134.
- (37) Cui, Y., Yang, F., Cao, X., Yarov-Yarovoy, V., Wang, K., and Zheng, J. (2012) Selective Disruption of High Sensitivity Heat Activation but Not Capsaicin Activation of TRPV1 Channels by Pore Turret Mutations. *J. Gen. Physiol.* 139 (4), 273–283.
- (38) Gibson, D. D. G., Young, L., Chuang, R. R.-Y., Venter, J. C., Hutchison, C. A., and Smith, H. O. (2009) Enzymatic Assembly of DNA Molecules up to Several Hundred Kilobases. *Nat. Methods* 6 (5), 343–345.